Modified Droop-based Fault Current Control for Grid Forming Converter during Network Faults

Irene Henry Masenge, *Student Member, IEEE,* Lie Xu, *Senior member, IEEE*, Yin Chen, and Agustí Egea-Àlvarez, *Member, IEEE*
Department of Electronic and Electrical Engineering
University of Strathclyde
Glasgow, UK
irene.masenge@strath.ac.uk, lie.xu@strath.ac.uk , yin.chen.101@strath.ac.uk , agusti.egea@strath.ac.uk

Abstract—**Reliability and stability of a power system are important aspects for the recent increase in inverter-based resources. Grid forming (GFM) converters have shown to be suitable solution as they can replicate the performance of a synchronous generator. However, since these converters have a characteristic of controlled voltage source behind impedance, they experience overcurrent during network faults. Recent research works have investigated the current limitation of GFM converters, however there is still a gap in the area. In this paper, a droop based GFM control is adopted, and its control is modified to support fault-ride through (FRT) strategy. An enhanced FRT method that switches to current control is implemented that improves the performance of GFM converter. The performance of the proposed technique is verified and validated through simulations in PSCAD/EMTDC.**

Keywords— Fault ride-through, current limitation, grid faults, voltage source converter, grid forming control.

I. Introduction

Voltage source converters (VSCs) which are widely used to integrate renewable power plants are crucial components that researchers have been researching on. The increase of the inverter based resources (IBRs) in the power network has reduced its transient voltage control ability [1]. Most of these IBRs adopt the grid following (GFL) control with a phase-locked loop (PLL) used to synchronize with the grid's frequency and phase.[2]. However, the control relies on a stiff voltage, such that during weak-grid and grid faults conditions, loss of synchronization and low frequency oscillations have been observed [3]. Compared to GFL control, grid-forming (GFM) control mimic traditional synchronous generators (SGs) and is able to maintain synchronization and voltage stability in weak grid conditions [4] . This has led to increased research interest in GFM control. However, unlike SGs, VSCs cannot inject high short-circuit currents (up to 6–8 pu) [5]. Therefore, a current limitation strategy is essential to protect the converters and enhance the reliability of the power grid during network transients, such as faults [6]. This is particularly critical for GFM converters, which operate as voltage sources under normal conditions. Implementing an effective current limiting strategy is then one of the important aspects in converter control.

Researches have shown that using virtual impedance (VI) for limiting converter currents and switching the control to current saturation algorithm (CSA) or GFL mode are the main fault-ride through (FRT) strategies [5] [6]. Instability has been observed when limiting current references directly due to winding up of outer power loops. In [6], it is shown that the problem can be solved through virtual impedance (VI) technique. However, it has been shown that in the first 25 ms the VI based FRT still experience overcurrent [7]. On the other hand, the study shows that in the first milliseconds after fault occurrence, the CSA based FRT has good current limiting capability. However, exiting the current saturation mode in the CSA FRT is still a problem that needs to be addressed. A study in [8] proposed an improved current limiting strategy that address the issue of postfault recovery from current saturation mode but the strategy is complex.

Grid codes require that active and reactive power are controlled during faults to enhance grid stability, reliability and prevention of power oscillations. For the VI FRT strategy, the angle of the GFM voltage is not aligned with the d-axis during faults. As a result, both the d-axis and q-axis currents influence reactive power, making it challenging to accurately control both active and reactive power in accordance with grid code requirements [9]. In contrast, the current saturation algorithm can directly and effectively limit the current and control reactive power during faults. However, for the current limitation strategy to be effective, accurate phase tracking is crucial. In [5] the potential instability phenomenon in droop-controlled GFM VSCs during faults is observed. The study introduced the *q-axis* component of the VSC voltage to the *P-f* droop control. However, to attain the control goal, the voltage needs to be aligned to the *d–axis* by the voltage control loop in steady state. [10] proposes a FRT method that switches from virtual synchronous generator (VSG) control to PLL based current control. However, it is not mentioned how the positional relationship between the VSG and PLL synchronous coordinate system is dealt with. Another study in [11] proposes a pre-synchronization method after studying positional relationships between different coordinate systems, however, the synchronization method still needs to be switched. A study in [8] proposes a hybrid synchronization control (HSC) strategy that effectively improves the transient stability margin of GFM VSCs by combining the *P-f* synchronization control and the PLL characteristics. However, the current limitation strategy used is complex. Moreover, synchronization is enhanced when a HSC is incorporated in the droop based GFM VSC with a LPF through reducing the active power reference as observed in [12]. However, inaccurate active power reference tracking is

observed. It can be seen that, modification of the active power control of the GFM VSC for enhancing synchronisation during network faults remains an open issue. Moreover, there is still a need for effective strategies to address the synchronization issues on the event of faults and the recovery after faults.

In this paper, a modified droop-based GFM is adopted to enhance synchronisation of GFM VSC when connected to the grid during network faults. The approach is used along with enhanced current limitation strategy that switches to current control to ride through faults. The approach doesn't require a backup PLL for synchronization and as previous studies have shown, the approach enhances synchronization of GFM VSCs on faults. Moreover the current limitation strategy used in this study is simple and shows good performance during and after the fault is being cleared.

The rest of the paper is structured as follows. Section II describes the control structure of basic GFM converter. The modified droop-controlled GFM converter together with the FRT strategy are described in Section III. Subsequently, to verify the effectiveness of the proposed strategy with the FRT strategy, the simulation results are shown in Section IV. Finally, Section V concludes the paper.

II. GRID-FORMING CONVERTER STRUCTURE

The system under study is depicted in Fig. 1. The grid is emulated by an ideal voltage source v_g behind an impedance, which is coupled to the converter point of common coupling (PCC) through transformers (T_1 and T_2) and transmission lines with impedance of Z_l. The converter system is then connected to the PCC through a linking inductance L and step-up transformer T_3. The study assumes a constant DC-link voltage V_{dc}. v_c and v_o are the converter terminal voltage and output voltage, respectively, and i_o is the converter output current.
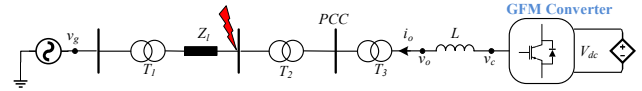

Fig. 1. System under study

The droop based GFM converter control structure is shown in Fig. 2. The power control loop is designed based on the *P-f* and *Q-V* droop GFM control with low pass filter (LPF) added to realize virtual inertia [13]. The *P-f* and *Q-V* droop control together form the inner virtual electromotive force (EMF), E of the virtual machine. The voltage magnitude E from the *Q-V* droop gives the reference voltage v_{od}^* that goes into the voltage and current control loops to generate the required converter output voltage V_{conv}. The *P-f* and *Q-V* droop control incorporates the LPFs to emulate inertial response of SGs [14]. The droop controllers can mathematically be expressed as:

$$\omega = \omega_o + m_p \cdot \frac{\omega_{cp}}{s + \omega_{cp}} \cdot (P^* - P) \qquad (1)$$

$$E = V_r + m_q \cdot \frac{\omega_{cq}}{s + \omega_{cq}} \cdot (Q^* - Q) \qquad (2)$$

where ω is the frequency of the output voltage, ω_o is the nominal frequency of the system. P^* and Q^* are the reference active and reactive power, respectively, while P and Q are the output active and reactive power, respectively. m_p and m_q are the active and reactive droop gains, respectively, whereas ω_{cp} and ω_{cq} are the cutoff frequencies of LPFs in the active and reactive loop, respectively. E is the amplitude of the electromotive force, and V_r is the rated voltage amplitude.
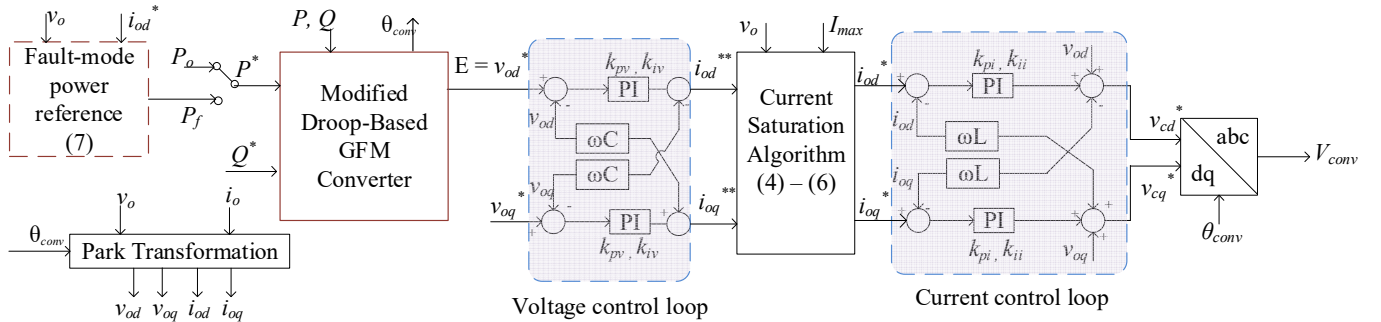

Fig. 2. Droop based GFM converter control

III. THE MODIFIED DROOP-CONTROLLED GFM CONVERTER AND CURRENT CONTROL STRATEGY

A. The Modified Droop-controlled GFM Converter

During faults it is necessary to control current to protect the converter semiconductor devices. However, precise control of active and reactive power as per grid code is also required, but is difficult to achieve with GFM control since the internal voltage angle is not aligned to the network voltage. Studies presented in [5] [12] and [8] show that during FRT,

the angle can be aligned through hybrid synchronization control. The control involves a q-axis component that is added through a proportional and integral controller (PI), which is similar to a conventional PLL, to the conventional *P-f* droop control.

To retain the *P-f* control during fault and to assist fault recovery, it is necessary to act on the outer power loop for appropriate phase and voltage references to properly control the *dq* axis current components. The *q-axis* component of

VSC voltage, i.e., v_{oq} that is added to the active power loop acts on the phase angle to ensure proper synchronisation during fault, as shown in Fig. 3. The added frequency deviation from v_{oq} can be expressed as:

$$\Delta\omega_{vq} = \left(k_{p\_pll} + \frac{k_{i\_pll}}{s}\right)v_{oq} \qquad (3)$$

where v_{oq} is the q-axis component of output voltage v_o, k_{p_pll} and k_{i_pll} are the proportional and integral gains of a PI controller that are used to ensure that $v_{oq} = 0$ during disturbances such as faults.

B. Enhanced Current Limitation Strategy

Power electronic devices need to be protected from overcurrent that result from faults in the network. Hence a current limiting strategy needs to be incorporated in the GFM VSC control. It is well known that provision of reactive current during faults is one of essential requirements by grid codes to assist recovery of voltage and for system stability [15]. The current limitation strategy in this study is as shown in Fig. 4 and it involves switching of the GFM control to current control where the current references are given by:

$$I_{oq}^* = \begin{cases} I_{oq}^{**} & 0.9 \le V_o \le 1.1 \\ -2(-V_o + 1) & otherwise \end{cases} \qquad (4)$$

$$I_{od}^* = \begin{cases} I_{od}^{**} & 0.9 \le V_o \le 1.1 \\ min(I_{d\_lim}, I_{d\_av}) & otherwise \end{cases} \qquad (5)$$

$$\text{where } I_{d\_lim} = \sqrt{I_{max}^2 - I_{oq}^{*2}}, \qquad (6)$$

$$I_{d\_av} = P_o/V_o$$

where $I_{max} = 1.2\,pu$ is the converter current limit, I_{d_av} is the available active current depending on the available nominal active power P_o on fault instance.

As the current references are limited, the integrator of the voltage control loop is reset to avoid the voltage control output from increasing. This is because the voltage control loops do not participate in vector current control when current is limited.

Moreover, as the current is being limited during fault, the active power refence needs to be scaled to reflect what is happening in the inner loops. This is essential so that the power synchronization loop can continue to work to give the desired angle during the fault. In addition to the benefit of angle alignment that is obtained from the modified droop control, active power reference is also reduced [12]. Then, scaling the active power reference according to the obtained active current reference I_{od}^*, will update the new active power reference to be:

$$P^* = P_f = I_{od}^* V_o \qquad (7)$$

After the fault is cleared, the parameters at the PCC are monitored to ensure that the normal grid conditions are restored (nominal voltage should be at least 0.9 pu). Considering slower dynamics of GFM control, as the control mode switches back to GFM on fault recovery, it is important

to carefully consider a switching delay to ensure smooth recovery. As discussed in the simulation results section, it is desired that the control switches back to GFM in a shorter delay time so that the GFM benefits can be regained. In this study a delay of 30 ms is chosen which shows better performance as discussed in the simulation results section.
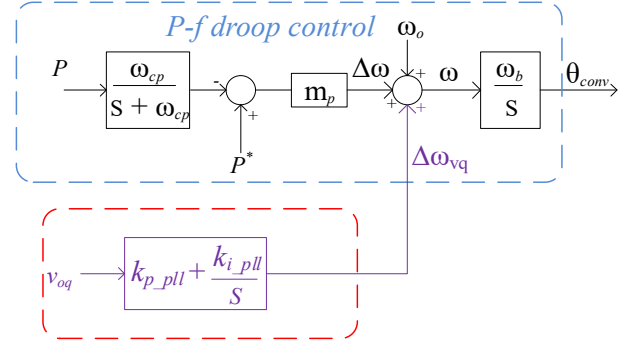

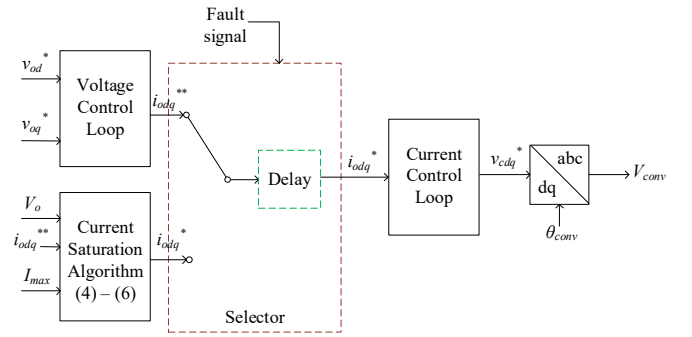Fig. 3. The Modified droop-based GFM converter control

Fig. 4. Enhanced Current Limitation Strategy

IV. SIMULATION RESULTS

The performance of the proposed modified droop control is tested through simulations in PSCAD/EMTDC. Table I shows the simulation parameters of the system. A symmetrical fault that lasts for 100 ms and causes the voltage to drop to about 50% of nominal voltage is applied at $2\,s$. The simulated response of the modified droop-based fault current control is observed when the control is immediately switched back from GFL to GFM after the fault clearance (when the AC voltage is recovered to at least 0.9 pu) and when the delays of 30 ms and 50 ms are considered. A more severe fault is also applied for the chosen switching delay of 30 ms that shows the good performance of the proposed strategy.

Fig. 5 shows the simulation results with the modified droop control, while the control is immediately switched back from GFL to GFM after the fault clearance. It can be observed in Fig. 5 (a) and (b) that during fault, voltage is being supported and current limited to $1.2\,pu$. Also, Fig. 5 (c) shows the dq-current components that are provided according to grid codes as in (4)-(6).

It is observed also in Fig. 5 (d) that during fault the voltage component v_{oq} is controlled precisely to zero to align the

voltage phasor to the *d-axis* to enhance synchronization which is made possible by the modified droop-based control. Moreover, Fig. 5 (e) shows the active and reactive power provided by the converter with active power delivered according to (*7*). However, switching back to GFM immediately after fault recovery results in poor postfault performance. It also takes about 100 ms for the voltage component v_{oq} to return to zero after fault is cleared as seen in, Fig. 5 (d).

TABLE I. MAIN SYSTEM PARAMETERS

Parameter	Value	Parameter	Value
Nominal l-l voltage V_n	6.6 kV	Cutoff frequency ω_{cp}, ω_{cq}	62.8 rad/s, 0.628 rad/s
Rated converter power S_n	400 MVA	Active droop gain m_p	0.02
Rated frequency f_o	50 Hz	Reactive droop gain m_q	0.001
Linking inductance L	0.15 pu	Gains k_{p_pll}, k_{i_pll}	950, 1900
Network transformer T_1,	400/132 kV	Voltage loop gains k_{pv}, k_{iv}	1, 350
Network transformer T_2	132/33 kV	Current loop gains k_{pi}, k_{ii}	1.35, 47.13
Network transformer T_3	33/6.6 kV	Fault recovery delay	30 ms

Fig. 6 shows the simulated response of the proposed strategy when a delay of 30 ms is applied for switching the control from GFL to GFM on fault recovery. It can be observed that during fault there is similar response to that in Fig. 5. On fault recovery, the response in Fig. 6 is significantly improved compared to that shown in Fig. 5. As seen in Fig. 6 (d), it takes about 20 ms for the voltage component v_{oq} to return to zero after fault clearance. The PCC voltage and current waveforms as seen in Fig. 6 (a) and (b) are also improved when compared to Fig. 5 (a) and (b).

Fig. 7 shows the simulated response of the proposed strategy when a delay of 50 ms is applied on the switching of the control from GFL to GFM. During fault, the response is similar to that shown in Fig. 5 and Fig. 6. On fault recovery, the response is comparable to that in Fig. 6 with 30 ms control switching delay. There is also no distortion in the PCC voltage and current waveforms that were observed in Fig. 5

The results in Fig. 5 to Fig. 7 show that a delay is essential on fault recovery, for smooth control switching from GFL to GFM. As GFM control offers more benefits compared to GFL control, it is desired that the control can switch back to GFM in a shorter delay time. Then a delay of 30 ms is selected.

Fig. 8 shows a more severe case where the voltage drops to about 0.2 pu during fault and with the delay of 30 ms applied when switching back to GFM control on fault recovery. It can be observed that during fault the voltage is supported and current limited to 1.2 pu. Also, the voltage

component v_{oq} is controlled precisely to zero to align the voltage phasor to the *d-axis*. Moreover, the active and reactive currents are provided according to *(4)-(6)* as shown in Fig. 8 (c). Also, the active and reactive power are provided according to with active power delivered according *(7)* as shown in Fig. 8 (e). The fault recovery is acceptable as the active power recovers to 90% of prefault value in 120 ms (the Great Britain grid code requires that in 0.5 s of fault clearance, active power to be restored to 90% of the pre-fault value). It also takes about 30 ms for the voltage component v_{oq} to return to zero after fault is cleared as seen in Fig. 8 (d).
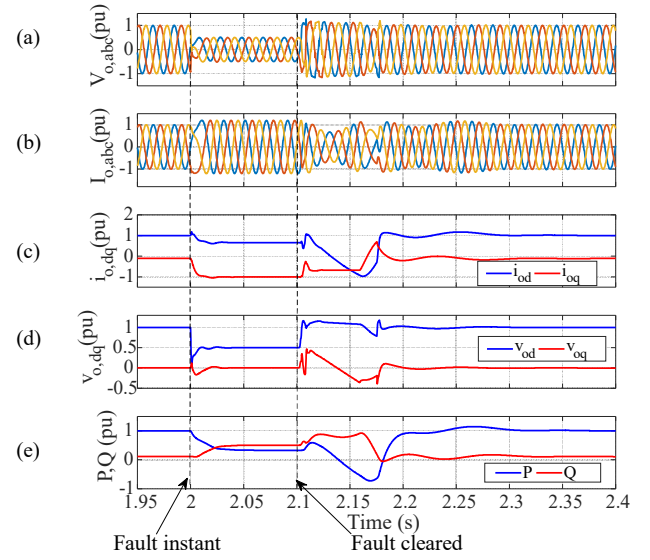

Fig. 5. Simulated response of the modified droop-based fault current control when no delay is applied on fault recovery.(a) Three-phase voltage at PCC. (b) Three-phase current at PCC. (c) dq-components of grid current. (d) dq-components of grid voltage. (e) Active and reactive power at PCC.
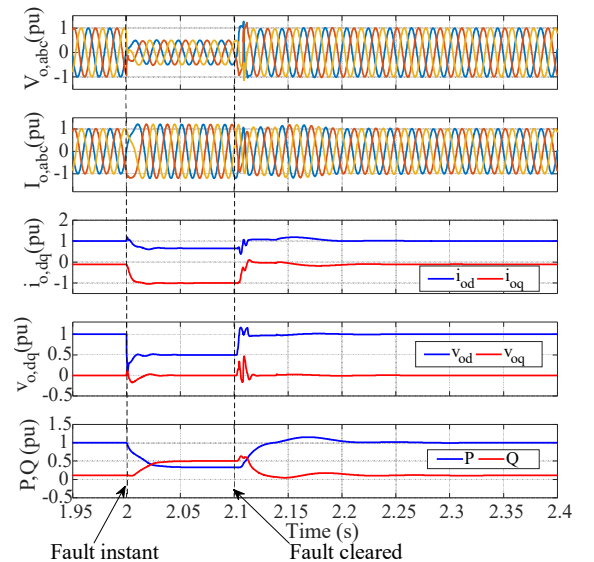

Fig. 6 Simulated response of the modified droop-based fault current control when a delay of 30 ms is applied on fault recovery.(a) Three-phase voltage at PCC. (b) Three-phase current at PCC. (c) dq-components of grid current (d) dq- components of grid voltage. (e) Active and reactive power at PCC.
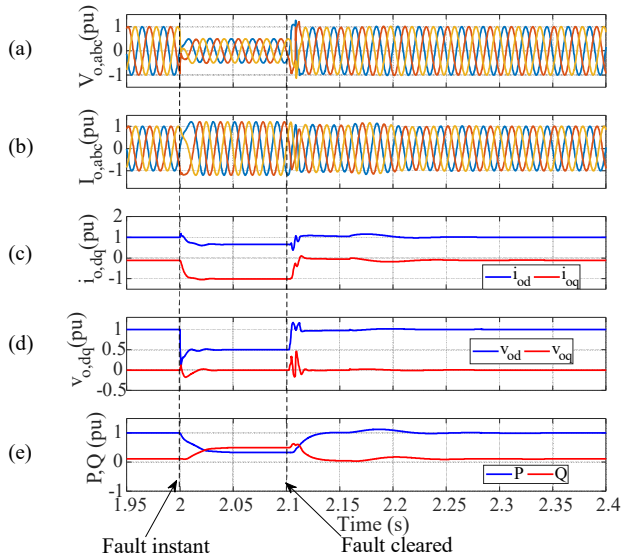
Fig. 7. Simulated response of the modified droop-based fault current control when a delay of 50 ms is applied on fault recovery.(a) Three-phase voltage at PCC. (b) Three-phase current at PCC. (c) dq-components of grid current. (d) dq- components of grid voltage. (e) Active and reactive power at PCC.
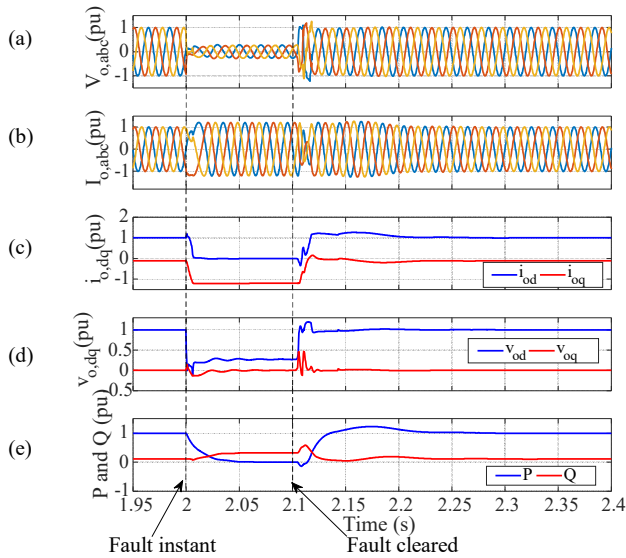

Fig. 8. Simulated response of the modified droop-based fault current control when a more severe fault is applied with a delay of 30 ms on fault recovery.(a) Three-phase voltage at PCC. (b) Three-phase current at PCC. (c) dq-components of grid current. (d) dq- components of grid voltage. (e) Active and reactive power at PCC.

V. CONCLUSION

This paper proposes a modified droop-based fault current control that uses the benefits of hybrid synchronisation control and proposes an enhanced current limiting strategy. It is observed that the proposed strategy improves the performance of GFM VSC by ensuring that during fault there is proper synchronization and the reactive current is provided as per grid code. Also the enhanced current limiting strategy is simple and has shown good performance. It is also worth mentioning that with the proposed technique, there is no need of backup phase locked loop (PLL) for synchronisation. The effectiveness of the proposed control strategy is validated through simulations in PSCAD/EMTDC.

REFERENCES

[1] J. Lyu, B. Liu, W. Zhang, and H. Yang, "Stability Analysis and Control Optimization Method for Symmetrical PLL-Based VSC in Weak Grid," in 2022 IEEE International Power Electronics and Application Conference and Exposition (PEAC), 2022: IEEE, pp. 1608-1614.

[2] P. Rodríguez, J. Pou, J. Bergas, J. I. Candela, R. P. Burgos, and D. Boroyevich, "Decoupled double synchronous reference frame PLL for power converters control," IEEE Transactions on Power Electronics, vol. 22, no. 2, pp. 584-592, 2007.

[3] M. G. Taul, X. Wang, P. Davari, and F. Blaabjerg, "An overview of assessment methods for synchronization stability of grid-connected converters under severe symmetrical grid faults," IEEE Transactions on Power Electronics, vol. 34, no. 10, pp. 9655-9670, 2019.

[4] Y. Li, Y. Gu, and T. C. Green, "Revisiting grid-forming and grid-following inverters: A duality theory," IEEE Transactions on Power Systems, vol. 37, no. 6, pp. 4541-4554, 2022.

[5] L. Huang, H. Xin, Z. Wang, L. Zhang, K. Wu, and J. Hu, "Transient stability analysis and control design of droop-controlled voltage source converters considering current limitation," IEEE Transactions on Smart Grid, vol. 10, no. 1, pp. 578-591, 2017.

[6] A. D. Paquette and D. M. Divan, "Virtual impedance current limiting for inverters in microgrids with synchronous generators," IEEE Transactions on Industry Applications, vol. 51, no. 2, pp. 1630-1638, 2014.

[7] T. Qoria, F. Gruson, F. Colas, X. Kestelyn, and X. Guillaud, "Current limiting algorithms and transient stability analysis of grid-forming VSCs," Electric Power Systems Research, vol. 189, p. 106726, 2020.

[8] P. Hu, W. Jiang, Y. Yu, D. Jiang, and J. M. Guerrero, "Transient stability improvement of grid-forming voltage source converters considering current limitation," Sustainable Energy Technologies and Assessments, vol. 54, p. 102839, 2022.

[9] R. Luo, H. Gao, F. Peng, and Y. Guo, "An Adaptive Low-Voltage Ride-Through Method for Virtual Synchronous Generators During Asymmetrical Grid Faults," IEEE Transactions on Sustainable Energy, 2024.

[10] H. Wu and X. Wang, "A mode-adaptive power-angle control method for transient stability enhancement of virtual synchronous generators," IEEE journal of emerging and selected topics in power electronics, vol. 8, no. 2, pp. 1034-1049, 2020.

[11] C. Shen et al., "Transient stability and current injection design of paralleled current-controlled VSCs and virtual synchronous generators," IEEE Transactions on Smart Grid, vol. 12, no. 2, pp. 1118-1134, 2020.

[12] T. Liu and X. Wang, "Physical insight into hybrid-synchronization-controlled grid-forming inverters under large disturbances," IEEE Transactions on Power Electronics, vol. 37, no. 10, pp. 11475-11480, 2022.

[13] J. Liu, Y. Miura, and T. Ise, "Comparison of dynamic characteristics between virtual synchronous generator and droop control in inverter-based distributed generators," IEEE Transactions on Power Electronics, vol. 31, no. 5, pp. 3600-3611, 2015.

[14] D. Pan, X. Wang, F. Liu, and R. Shi, "Transient stability of voltage-source converters with grid-forming control: A design-oriented study," IEEE Journal of Emerging and Selected Topics in Power Electronics, vol. 8, no. 2, pp. 1019-1033, 2019.

[15] K. H. Oon, C. Tan, A. Bakar, H. S. Che, H. Mokhlis, and H. Illias, "Establishment of fault current characteristics for solar photovoltaic generator considering low voltage ride through and reactive current injection requirement," Renewable and Sustainable Energy Reviews, vol. 92, pp. 478-488, 2018.